Chaos and Locking in a Semiconductor Laser Due to External Injection

V. Annovazzi-Lodi, *Member, IEEE*, S. Donati, *Member, IEEE*, and M. Manna

***Abstract*—We have analyzed the behavior of a semiconductor laser subjected to increasing external injection. Numerical simulations show the well-known nonlinear modulation and locking regimes, followed by an intermediate chaotic region that precedes definitive locking to the external source at significantly higher injection levels.**

I. Introduction

In the last years, considerable attention has been devoted to coupling phenomena in laser sources. Both symmetrical and asymmetrical coupling (representative of external injection) have been analyzed, showing that at increasing levels of exchanged power, the oscillation undergoes a regime of amplitude and frequency nonlinear modulation before locking [1].

The particular case of self-coupling, usually referred to as optical feedback, has been extensively studied [2]–[9] because of its importance in connection with frequency-stabilized lasers. It has been shown that high levels of feedback can lead to instability and chaos in both semiconductor and gas lasers.

More recently [9], instability and chaos have also been reported for the injection scheme, which is representative, for instance, of a master/slave synchronized pair or of a local oscillator detection system. Injection has also been proposed as a tool for determining fundamental parameters of a laser [10].

In this paper, we focus our attention on the injection scheme to study the evolution toward, inside, and beyond the chaotic region. We find that the system finally reaches a locked regime at a level of injection much higher than the level of the first locking event, which precedes the intermediate chaotic region.

II. Analysis of the Injection Regime

In the following, we will analyze the basic scheme of Fig. 1, where a signal of constant amplitude E_s and frequency ω_s is injected into a monomode semiconductor laser source of internal amplitude E_0.

External injection in a semiconductor laser is described by adding a suitable forcing term to the standard laser equations derived by Lang and Kobayashi [2], [5], [11], [12]. For the injection scheme, the delayed term $Ee^{j\omega(t-\tau)}$ for the reflection at a remote mirror is replaced [9] by $E_s e^{j\omega_s t}$ expressing the electric field injected by the external source. Letting $E(t) = E_0(t)\, e^{j[\omega t + \phi(t)]}$ and writing separate equations for amplitude and phase, we get

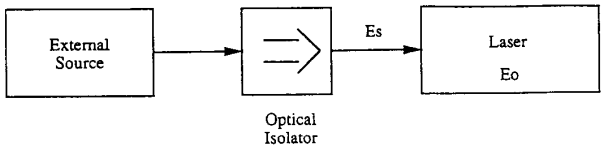

Fig. 1. Scheme of unilateral injection coupling between laser sources.

$$\frac{dE_0}{dt} = \frac{1}{2}\left\{G_n(N - N_0)(1 - \epsilon\Gamma E_0^2) - \frac{1}{\tau_p}\right\} E_0 + \frac{K}{\tau_{\text{in}}} E_s \cos\psi(t) \tag{1a}$$

$$\frac{d\psi}{dt} = \frac{1}{2}\, a^* \left\{G_n(N - N_0)(1 - \epsilon\Gamma E_0^2) - \frac{1}{\tau_p}\right\} - \frac{K}{\tau_{\text{in}}} \frac{E_s}{E_0(t)} \sin\psi(t) - \Delta\omega_s \tag{1b}$$

$$\frac{dN}{dt} = Rp - \frac{N}{\tau_r} - G_n(N - N_0)(1 - \epsilon\Gamma E_0^2) E_0^2. \tag{1c}$$

In (1a)–(1c), the usual notation is assumed [2], [5], i.e.:

- N is the carrier concentration and N_0 is its value at the inversion threshold;
- G_n is the modal gain;
- $\psi(t) = \phi(t) - \Delta\omega_s t$ is the phase difference between the internal and the injected fields;
- $\Delta\omega_s = \omega_s - \omega_0$ is the frequency difference between the external signal and the unperturbed laser oscillation;
- τ_p is the photon lifetime in the cavity;
- τ_r is the electron/hole recombination time;
- $\tau_{\text{in}} = 2L/c$ is the time of flight in the laser cavity of length L;
- $\epsilon\Gamma$ is the product of compression and of confinement factors;
- $R_p = J\eta/ed$ is the pump parameter that depends on supply current density J, efficiency η, and active region thickness d;

Manuscript received November 6, 1992; revised December 9, 1993. This work was supported by a MURST-40% Contract.

The authors are with the Dipartimento di Elettronica, Universita' di Pavia, Pavia, Italy.

IEEE Log Number 9401164.

$a^* = -2\omega_0/(n^*G_n)\ \partial n/\partial N$;

$n^* = n + \omega_0\ \partial n/\partial\omega$ is an effective refractive index, and

K is the injection parameter, defined as the field attenuation experienced by the external signal E_s up to the superposition on E_0.

As in previous papers, in (1a)–(1c), E_0 is a normalized electric field, i.e.:

$$E_{0\text{true}} = E_0\left[G_n \frac{h}{2\pi}\,\omega\,\frac{Z_0}{\sigma n}\right]^{1/2}$$

where σ is the laser stimulated emission cross section, n is the refractive index, and Z_0 is the impedance of vacuum.

This model is valid for small detuning, i.e., $\Delta\omega_s < \Delta\omega_c$, where $\Delta\omega_c$ is the cavity linewidth.

To select a typical case of injection into a semiconductor laser, we have assumed an output power $P_0 = 1$ mW and a consistent set of values for the parameters as in [8], i.e.:

$G_n = 8.1 \cdot 10^{-13}\ \text{m}^3/\text{s}$; $N_0 = 1.1 \cdot 10^{24}\ \text{m}^{-3}$;

$\omega = 2.5133 \cdot 10^{15}\ \text{rad} \cdot \text{s}^{-1}$; $\tau_p = 2 \cdot 10^{-12}$ s;

$\tau_r = 2 \cdot 10^{-9}$ s; $\tau_{\text{in}} = 8 \cdot 10^{-12}$ s;

$\epsilon\Gamma = 9 \cdot 10^{-24}\ \text{m}^{-3}$; $a^* = 6$;

$R_p = 9.075 \cdot 10^{32}\ \text{m}^{-3}/\text{s}^{-1}$; $E_s = 1.02 \cdot 10^{10}\ \text{m}^{-3/2}$ $[\approx E_0(K = 0)]$.

Equation (1a)–(1c) has been integrated by a standard computer routine. In the calculation, we took E_s as a constant and varied K to adjust the injection level. The adimensional factor K has been found to be a suitable order parameter in the transition to chaos, as will be clear in the following.

We have computed about 1000 simulations at various K and $\Delta\omega_s$ to follow the system evolution through the regimes of weak modulation, multiperiodicity, chaos, and locking.

In Figs. 2–5 we report the evolution for a specific detuning, i.e., $\Delta\nu_s = \Delta\omega_s/2\pi = 36$ MHz, and for a range of the injection parameter K spanning from the unperturbed regime ($K = 0$) to the final locking (a few 10^{-2}). The selected $\Delta\omega_s$ value can be considered as a moderate detuning but is representative of a wide range of $\Delta\omega_s$.

The system route to chaos is illustrated by the bifurcation diagram in which the ordinates represent the intersections of the phase-plane curve (dE_0/dt versus E_0) with the semiaxis $E_0 > E_0^*$, where $E_0^* = E_0(K = 0)$. The bifurcation diagram obtained for weak injection levels is plotted in Fig. 2, and its general trend is in agreement with previously reported results [9]. We have also obtained the new results shown in Fig. 3 for moderate K, which shows a sequence of chaos and bifurcations in reverse order (with respect to Fig. 2) up to the final locking.

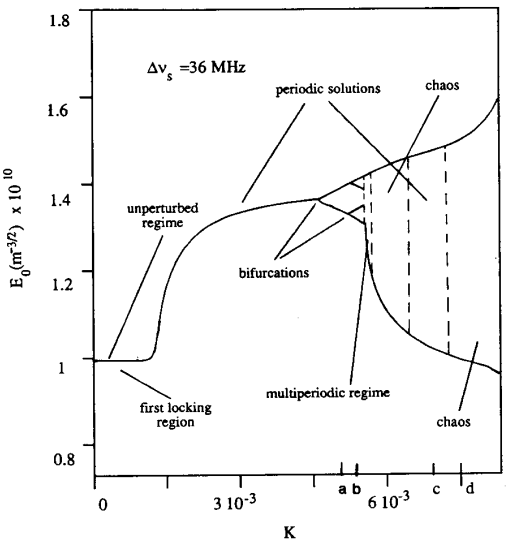

Fig. 2. Bifurcation diagram for weak injection in a semiconductor laser showing the route to chaos. The sequence of regimes entered at increasing K is labeled on the diagram. Selected points are indicated for (a) ($K = 5 \cdot 10^3$) first-period doubling; (b) ($5.3 \cdot 10^{-3}$) second-period doubling; (c) ($7 \cdot 10^{-3}$) periodicity inside a chaotic region; and (d) ($7.6 \cdot 10^{-3}$) chaos.

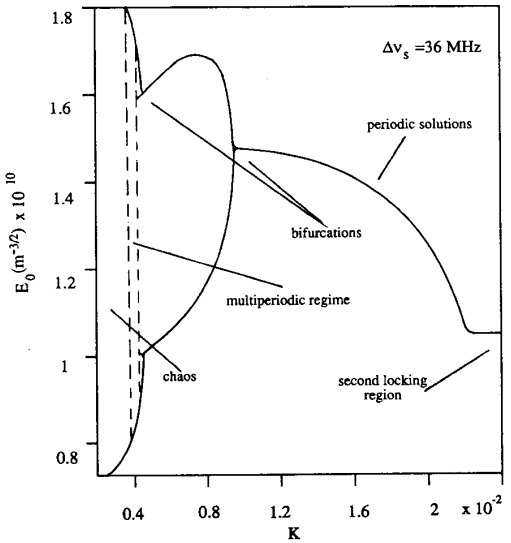

Fig. 3. Bifurcation diagram for a moderate injection showing the route from chaos to the final locking region.

In Figs. 4 and 5 (top line) we report the amplitude beating waveforms of E_0 and E_s, i.e., the signal obtained by photodetection of the laser beam. The waveforms are normalized to E_s and show the evolution from a sinusoid to an increasingly distorted waveform as the system becomes chaotic. Additional information is provided by the beating spectrum, which allows tracking of the onset of new subharmonics at each bifurcation and the transition from a line to a continuous spectrum as an indicator of chaos. This is shown in the middle row of Fig. 5.

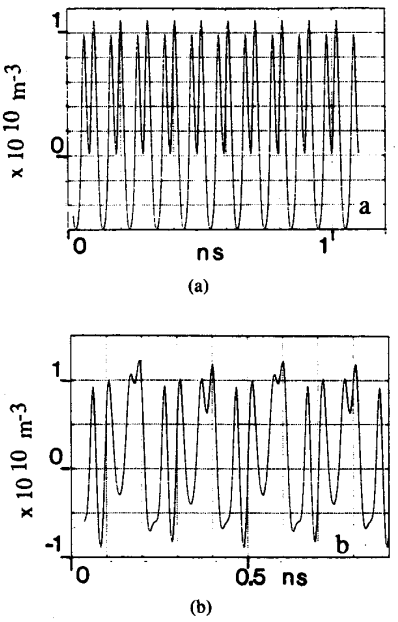

Fig. 4. Normalized beating waveforms $E_0 \cos \psi(t)$ for points (a) (top) and (b) (bottom) of Fig. 2.

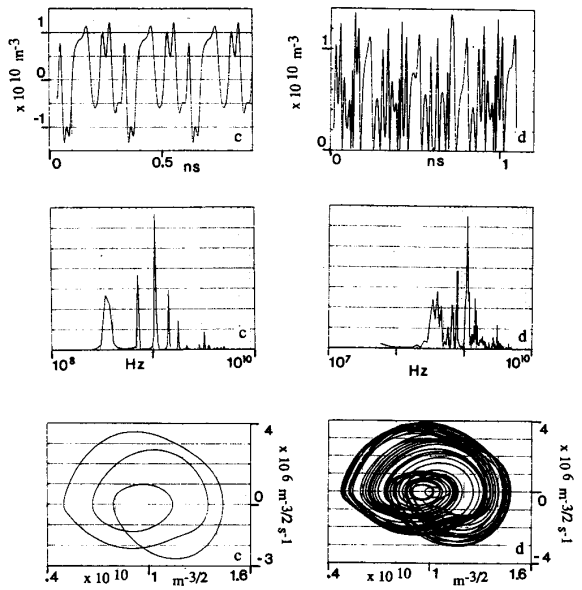

Fig. 5. Normalized beating waveforms $E_0 \cos \psi(t)$ (top line), beating power spectra (center), phase-plane diagrams dE_0/dt versus E_0 (bottom line) for points (c) (first column), and (d) (second column) of Fig. 2. The sharpness of the first peak spectrum (center left) at a relatively low frequency is limited by the resolution of the FFT routine.

Finally, phase-plane diagrams are reported in the last row of Fig. 5. This representation gives an immediate indication of the system degree of order. Splitting of the limit cycle is observed in such diagrams at each bifurcation, as well as the widening of the phase-plane diagram from a simple or folded closed curve to a figure covering a whole region of the plane, as the system is approaching chaos.

Let us describe in more detail the results of Figs. 2–5. Starting with very weak injection ($K < 10^{-4}$), the laser oscillation remains virtually unperturbed, and the beating waveform between the two sources is sinusoidal. For $K > 10^{-4}$, the laser enters the automodulation regime already described in [1], which consists of amplitude and frequency modulations whose depths increase with K. In this region, the beating waveform becomes increasingly distorted, and finally it becomes pulse-like, though it remains periodic; for most of the time the phase between the two lasers is almost constant, while in a short fraction of the period it turns to nearly 2π. Then, at an injection level of $K_1 = 5 \cdot 10^{-4}$ the laser locks in phase to the external source.

The above behavior is also correctly predicted in the well-known Adler's approximation [1], which disregards the time dependence of N and G_n expressed by (1c). However, the reduced set of (1a) and (1b) give, in this case, a larger locking value ($K_1 = 1.8 \cdot 10^{-3}$) and, more importantly, do not lead to the chaotic regime.

Going back to (1a)–(1c), it is found that beyond the first locking value, ($K > K_1$) the laser does not remain locked to the driving source (as predicted by the Adler's approximation), but it unlocks beyond a certain value of K ($K = 1.2 \cdot 10^{-3}$ in our case). The beating waveform is still periodic, and looks like a sinusoid with a second harmonic distortion (initially small), which gradually increases until for $K = 4.7 \cdot 10^{-3}$ the period doubles and the system enters a bifurcation cascade ($K = 4.7 \cdot 10^{-3}$, $5.2 \cdot 10^{-3}$, $\cdots$).

Fig. 4 shows the normalized beating waveforms of E_0 and E_s pertinent to points (a) and (b) of Fig. 2, i.e., just after the first and the second bifurcation. The diagrams clearly show the period doubling and the increasing distortion of beating. In this regime the phase-plane diagram is not a simple curve (i.e., it has one or more knots) but is still represented by a closed cycle composed of well-defined turns.

The bifurcations are followed by a narrow range of K (Fig. 2) in which a multiperiodic regime takes place. Here, the phase-plane diagram is no longer a regular curve; it becomes quite involved and covers a whole region of the plane; however, the beating signal still has a discrete spectrum and this allows discrimination against the chaotic regime.

Then, the system enters the chaotic region. Here, the beating waveform is not periodic and the phase-plane diagram covers a whole region of the plane. In addition, the signal spectrum broadens and becomes continuous. These features are typical of chaotic behavior and are shown in the diagrams of the second column of Fig. 5 corresponding to point (d) of Fig. 2. Here, the phase-plane diagram, the beating waveform, and its spectrum are often found to show abrupt changes after small variations of K.

As it is well known, in the chaotic region the long-term behavior of the system becomes unpredictable (or better

to say, only statistically predictable) and coherence is impaired. However, for narrow ranges around special values of K, the chaotic region embeds islands where the regime is again multiperiodic, or even periodic. This is, for example, the case of $K \approx 7 \cdot 10^{-3}$ (point (c) in Fig. 2) for which there are periodic solutions (of odd periodicity), as shown in the first column of Fig. 5.

At still higher levels of K, the chaotic regime breaks down to a sequence of evolution intervals reverting to more ordered regimes.

This fact is illustrated in Fig. 3, where we report the bifurcation diagram for relatively high K. It can be seen that the system instability is reduced for increasing K and that a route from chaos to locking is now followed. The system evolution described in this diagram comprises the same fundamental events, previously discussed and reported in Fig. 2, but in reverse order. In fact, for $K \approx 4 \cdot 10^{-2}$ we find a new region of multiperiodic solutions, followed by a reverse-order bifurcation cascade, where the branches of the bifurcation diagram merge for increasing K, until for $K = 4.3 \cdot 10^{-2}$ the diagram becomes double-valued and for $K = 9 \cdot 10^{-2}$ it becomes single-valued. From this point onward, the phase diagram is again a simple closed curve and beating approaches a sinusoid. The laser is in a periodic regime that lasts until $K \approx 0.25$. For this value the laser definitively locks to the external source, and any further increase of injected power does not result in any significative change of regime.

The bifurcation diagrams obtained for other values of detuning are essentially equivalent. For a wide range of $\Delta\omega_s$ ($5 \cdot 10^6$ to $6 \cdot 10^8$ rad/s), it was always found a route to chaos by bifurcations, including a few cases of third-order splitting (observed e.g., for $\Delta\nu_s = 12$ MHz, $\Delta\nu_s = 98$ MHz). Narrow regions of multiperiodicity were generally found inside the chaotic region. Two locking regions were always found, one for a relatively narrow range of injected power and the other for sufficiently high-power injection. In the above analysis we had to discriminate between chaos and multiperiodic regime. In some cases, the chaotic behavior was evident from inspection of the beating and its spectrum. In less evident cases, however, Lyapunov exponents [13] were calculated to discriminate between the two regimes.

For the numerical computations, we used both a 386-based personal computer with a 387 math coprocessor and a VAX-6410 mainframe computer. Typical elapsed CPU time for simulations such those reported in Figs. 3 and 4 ranged from 30 min to 1 h (VAX). The time resolution was initially set to 10^{-14} s and was automatically varied during computations after evaluating the derivatives of the state variables.

III. Conclusions

In summary, we have shown that a typical semiconductor laser can route to chaos due to external injection for a wide range of the coupling parameter; this fact is important in synchronization and coherent detection experiments. In addition, we have shown that transition to chaos does not prevent effective locking between sources. This fact, which has been verified for a wide range of parameters, is not surprising, as one should expect that for sufficiently high injected power the laser should finally lock to the injecting source. This is also in accordance with experimental work reported earlier in the literature, especially on gas lasers. However, it must be pointed out that Adler's approximation leads to a substantial underestimation of the minimum level of coupling that allows one to definitively achieve locking. This circumstance, apparently unnoticed in previous work, clearly has an important impact in many applications.

References

[1] V. Annovazzi-Lodi and S. Donati, "Injection modulation in coupled laser oscillators," *IEEE J. Quantum Electron.*, vol. QE-16, pp. 859–864, Aug. 1980.

[2] R. Lang and K. Kobayashi, "External optical feedback effects on semiconductor injection laser properties," *IEEE J. Quantum Electron.*, vol. QE-16, pp. 347–355, Mar. 1980.

[3] B. Tromborg, J. H. Osmundsen, and H. Olesen, "Stability analysis for a semiconductor laser in an external cavity," *IEEE J. Quantum Electron.*, vol. QE-20, pp. 1023–1033, Sept. 1984.

[4] J. Sacher, W. Elsässer, and E. Göbel, "Intermittency in the coherence collapse of a semiconductor laser with external feedback," *Phys. Rev. Lett.*, vol. 63, no. 20, pp. 2224–2227, Nov. 1989.

[5] B. Tromborg and J. Mørk, "Nonlinear injection locking dynamics and the onset of coherence collapse in external cavity lasers," *IEEE J. Quantum Electron.*, vol. QE-26, pp. 642–654, Apr. 1990.

[6] ——, "Stability analysis and route to chaos for laser diodes with optical feedback," *IEEE Photon. Technol. Lett.*, vol. 2, pp. 549–552, Aug. 1990.

[7] J. Sacher, W. Elsässer, and E. Göbel, "Nonlinear dynamics of semiconductor laser emission under variable feedback conditions," *IEEE J. Quantum Electron.*, vol. 27, pp. 373–379, Mar. 1991.

[8] J. Mørk, B. Tromborg, and J. Mark, "Chaos in semiconductor lasers with optical feedback: Theory and experiment," *IEEE J. Quantum Electronics*, vol. 28, pp. 93–107, Jan. 1992.

[9] J. Sacher, D. Baums, P. Panknin, W. Erlsässer, and O. Göbel, "Intensity instabilities of semiconductor lasers under current modulation, external light injection and delayed feedback," *Phys. Rev. A*, vol. 45, pp. 1893–1905, Feb. 1992.

[10] J. M. Liu and T. B. Simpson, "Characterization of fundamental parameters of a semiconductor laser with an injected optical probe," *IEEE Photon. Technol. Lett.*, vol. 4, pp. 380–382, Apr. 1993.

[11] R. Lang, "Injection locking properties of semiconductor lasers," *IEEE J. Quantum Electron.*, vol. QE-18, pp. 976–983, June 1982.

[12] B. Tromborg, H. Olesen, X. Pan, and S. Saito, "Transmission line description of optical feedback and injection locking for Fabry–Perot and DFB lasers," *IEEE J. Quantum Electron.*, vol. 23, pp. 1875–1889, Nov. 1987.

[13] H. G. Schuster, *Deterministic Chaos.* Weinheim: VCH Publishers, 1989.

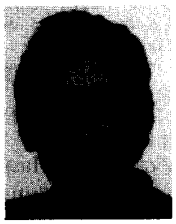

Valerio Annovazzi-Lodi (M'89) was born in Novara, Italy, on November 7, 1955. He received the degree in Electronic Engineering, cum laude, from the University of Pavia, Pavia, Italy, in 1979.

Since then he has been working at the Department of Electronics of the University of Pavia in the field of electrooptics, formerly on injection modulation phenomena in lasers and on the fiber gyroscope, and later on birefringence effects in optical fibers, fiber sensors, and transmission via diffused infrared radiation. In 1983 he became a staff researcher of the Department of Electronics of the University of Pavia and in 1992 he became an associate professor in the same institution.

Mr. Annovazzi-Lodi is a member of AEI.

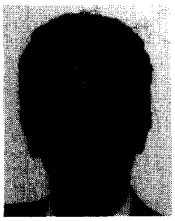

Silvano Donati (M'75) was born in Milano on August 19, 1942 and graduated in Physics cum laude at the University of Milano in 1966.

From 1966 to 1975 he was with CISE (Milano), carrying out research on noise in photomultipliers and avalanche photodiodes, nuclear electronics, and electrooptic instrumentation. In 1975 he joined University of Pavia, Department of Electronics, where he became full professor of Optoelectronics in 1980. He has worked on laser interferometry, fiber gyroscopes and noise in CCD's and, more recently, on optical fiber sensors, passive fiber components for telecommunications, and optical interconnections.

Dr. Donati has authored or coauthored about a hundred papers and holds three patents. He is a member of AEI, APS, OSA, ISHM, and has served to organize several national and international meetings and schools in steering and program committees or as a chairman. He also worked in the standardization activity of CEI/IED (CT-76 laser safety).

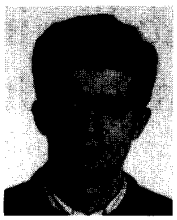

Massimo Manna was born in Lecco, Italy, on December 24, 1967. He received the degree in Electronic Engineering in 1992 from the University of Pavia, Italy. Upon graduation he worked for some month at the Electrooptics Laboratory in Pavia. In 1993 he joined Sgs-Thomson Microelectronics where he was a Device Engineer for microelectronic technology.

Since February 1994 he has been working as Reliability Engineer in the R&D group for optical amplifiers (EDFA) at Pirelli Cavi Spa, Milan, Italy.